

An Explanation for the Very Large Breathing Effect of a Metal–Organic Framework during CO₂ Adsorption**

By Christian Serre,* Sandrine Bourrelly, Alexandre Vimont, Naseem A. Ramsahye, Guillaume Maurin, Philip L. Llewellyn, Marco Daturi, Yaroslav Filinchuk, Olivier Leynaud, Paul Barnes, and Gérard Férey*

Breathing is usually associated with life. However, such a reversible process can also, intriguingly, be associated with solid-state materials that have the ability to ‘breathe’ when exposed to an external stimulus (e.g., pressure, temperature, light, gas, or solvent adsorption), sometimes with large variations (> 5 Å) in their unit-cell parameters. This phenomenon primarily occurs with porous solids containing a hybrid organic–inorganic framework because of the interaction of guest molecules with the host structure. Furthermore, it is often observed in the subclass of coordination polymers that combine inorganic clusters with organic linkers and in structures where the inorganic moi-

eties are 1D or 2D.^[1–6] Kitagawa and co-workers recently proposed categorizing the different behaviors into six classes according to the dimensionality of the inorganic subnetwork and the types of host–guest interactions. However, most of the literature to date has focused on the structure of the initial and final stages of the breathing solid through crystal-to-crystal transformations without seeking a physical explanation for this breathing effect. This Communication focuses on providing an answer to this unresolved issue for the case of CO₂ adsorption at room temperature for porous chromium(III) terephthalate MIL-53 [Cr^{III}(OH)(OOC–C₆H₄–COO)], which was discovered a few years ago.^[2,7]

The structural topology of MIL-53^[1,2,7] consists of a 4⁴ net (Fig. 1a) with tilted chains of Cr^{III}O₄(OH)₂ octahedra sharing

[*] Dr. C. Serre, Prof. G. Férey
Institute Lavoisier (UMR CNRS 8180)
Université de Versailles St-Quentin-en-Yvelines
45, Avenue des Etats-Unis
78035 Versailles Cedex (France)
E-mail: serre@chimie.uvsq.fr; ferey@chimie.uvsq.fr

S. Bourrelly, Dr. P. L. Llewellyn
MADIREL (UMR CNRS 6121)
Université de Provence
13397 Marseille Cedex 20 (France)

Dr. A. Vimont, Prof. M. Daturi
Laboratoire Catalyse et Spectrochimie (UMR CNRS 6506)
ENSICAEN-Bâtiment C
6 Boulevard Maréchal Juin
14050 Caen (France)

Dr. N. A. Ramsahye, Dr. G. Maurin
Institut Charles Gerhardt (UMR 5253 CNRS UM2 ENSCM)
Université de Montpellier II
34095 Montpellier Cedex 05 (France)

Dr. Y. Filinchuk
SNBL at ESRF, BP-220
38043 Grenoble (France)

Dr. O. Leynaud, Prof. P. Barnes
School of Crystallography
Birkbeck College
Malet Street
London WC1E 7HX (UK)

Dr. O. Leynaud, Prof. P. Barnes
Department of Chemistry
University College
20 Gordon Street
London WC1H 0AJ (UK)

[**] This work was supported by CNRS, EU funding via FP6-Specific Targeted Research Project “DeSANNs” (SES6-020133) and UK-EPSCRC funding. The authors are indebted to the Daresbury SRS and the ESRF in Grenoble for providing beamtime and the help of their staff during and after the experiments. Supporting Information is available online from Wiley InterScience or from the author.

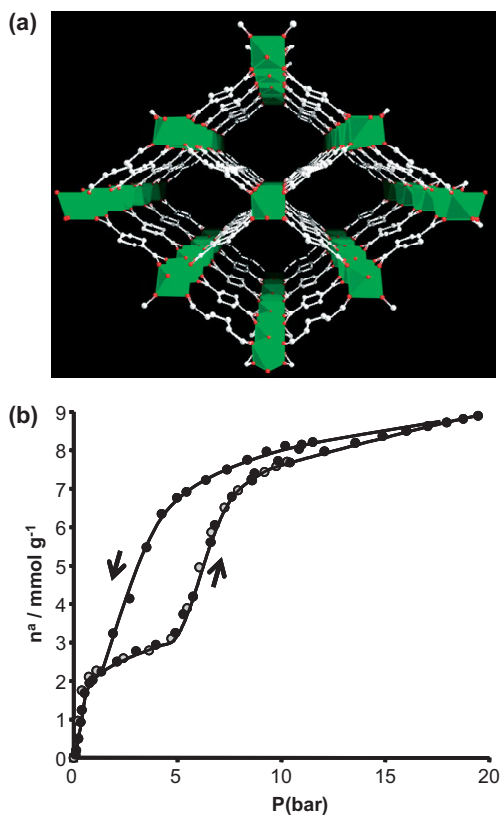


Figure 1. a) View of the structure of MIL-53HT along the *c*-axis (green: Cr, red: O, light gray: C). b) Adsorption–desorption isotherms of MIL-53(Cr) at 304 K.

trans hydroxyl groups solid (structural data: orthorhombic; space group, SG, Pnam; $a=17.340(1)$ Å, $b=12.178(1)$ Å, $c=6.822(1)$ Å; $V=1440.6(1)$ Å³). These chains are linked via the carboxylate groups of the terephthalate ions (1,4-benzene dicarboxylate, BTC), forming a 3D framework. 1D tunnels accommodate residual terephthalic acid moieties in the as-synthesized form, which can be removed by evacuation at 423 K, giving rise to a slight volume increase (orthorhombic; SG Imcm; $a=16.733(1)$ Å, $b=13.038(1)$ Å, $c=6.812(1)$ Å; $V=1486.2(2)$ Å³). The latter phase, MIL-53HT, where HT indicates high temperature, cooled at ambient pressure, reversibly adsorbs one water molecule per Cr atom, leading to a drastic shrinkage of the tunnel in the resulting MIL-53LT solid, where LT indicates low temperature, (monoclinic; SG C2/c; $a=19.685(4)$ Å, $b=7.849(1)$ Å, $c=6.782(1)$ Å, $\beta=104.90(1)^\circ$; $V=1012.8(1)$ Å³) corresponding to atomic movements larger than 5 Å. Despite the chemical changes, the structure remains topologically invariant.

For the isotopic Al-containing solid, an in situ solid-state NMR study^[8] of the hydration of MIL-53HT showed that the shrinkage that occurred upon insertion of water molecules resulted from the onset of two types of strong hydrogen bonds. The first type involves the hydrogen atoms of water molecules and the oxygen atoms of the bridging carboxylate groups. The second type, which seems to be more energetically favorable, links OH groups to inserted water molecules.

It has been recently shown that MIL-53 can absorb hydrogen at low temperature^[9] and a large amount of CO₂ at room temperature.^[10] The latter process proceeds in two steps (Fig. 1b): after a very fast uptake at low pressure (ca. 2–3 mmoles g⁻¹), the isotherm reaches its first plateau between 1 and 4 bar (1 bar = 100 000 Pa) followed by an adsorption of more than a double amount of CO₂ at higher pressures. Interestingly, desorption occurs with hysteresis, and the desorption branch returns to the adsorption branch at ca. 2 bar. This unusual effect was interpreted^[10] according to the following hypothesis. After activation of the hydrated material, the degassed solid exhibits an open structure. After the first portion of CO₂ is absorbed, the host–guest interactions force the framework to close and the cell to shrink. A further absorption of CO₂ at higher pressures reopens the framework while accepting additional CO₂ molecules into a newly formed tunnel (ca. 9–10 mmoles g⁻¹). This Communication presents experimental evidence for this hypothesis based on in situ diffraction experiments performed at synchrotron radiation facilities, including Daresbury Synchrotron Radiation Source (UK), where a qualitative model of the structural transformations was derived at 1–10 bar CO₂,

and at the European Synchrotron Radiation Facility (ESRF, France), where a structure of an intermediate phase at 1 bar, corresponding to the beginning of the plateau, was determined.

MIL-53(Cr) was synthesized as described previously.^[2] High-resolution data collected at ESRF on the activated sample verified, as expected, that the structure under vacuum corresponded to the open form of MIL-53HT (Fig. S1). Next, a set of in situ powder patterns were collected by using a rapid powder diffraction detector (RAPID2,^[11] beamline MPW6.2^[12] at Daresbury, UK) under CO₂ pressure. The data indicates that at 2 bar the resulting solid, MIL-53LP (where LP denotes low pressure) exhibited a similar diffraction pattern to MIL-53LT. In contrast, at 10 bar the resulting solid, MIL-53HP (where HP is high pressure) resembled the HT form of MIL-53, thereby confirming the structural expectations gained from the adsorption measurements (Fig. 2 and Fig. S1). Longer experiments that used increasing/decreasing stepwise changes in pressure showed that shrinkage also occurred at very low pressures and, moreover, confirmed the previously observed hysteresis. With decreasing pressure, MIL-53LP appeared below 2 bar; however, at increasing pressures, it assumed its predominant form up to 5 bar. The rapid opening and closing of the MIL-53 topology under CO₂ pressure indicated an excellent cycling ability of the breathing phenomenon in the presence of CO₂ gas (Fig. 3).

To explain the observed shrinkage of the unit cell upon absorption of the first portion of CO₂, we performed a detailed structural study of a sample obtained at the plateau pressure. High-resolution powder X-ray diffraction (XRD) data were collected at 195 K under 1 bar of CO₂ at Swiss–Norwegian Beamlines (ESRF) by using a gas-dosing system connected to a glass capillary. The resulting powder pattern was indexed in

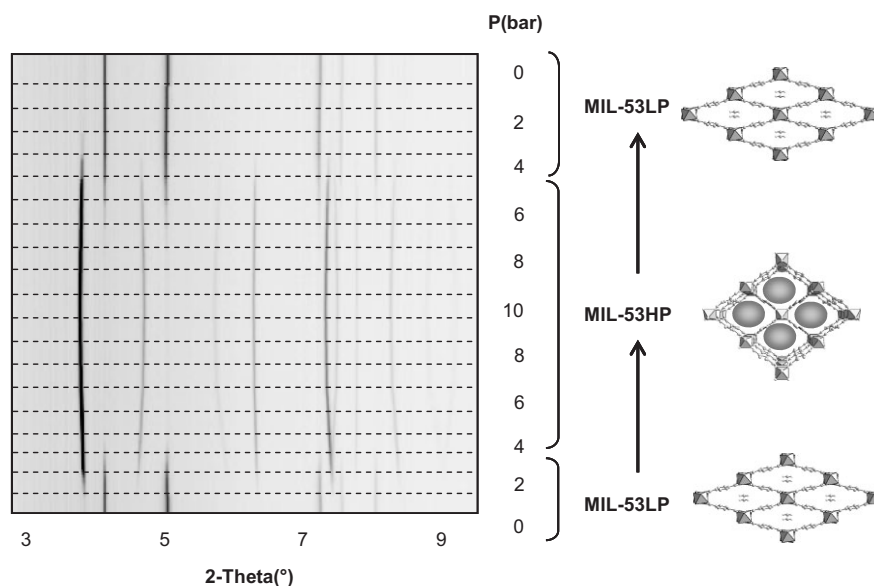


Figure 2. Powder XRD patterns of MIL-53(Cr) under various pressures of CO₂ at 293 K.

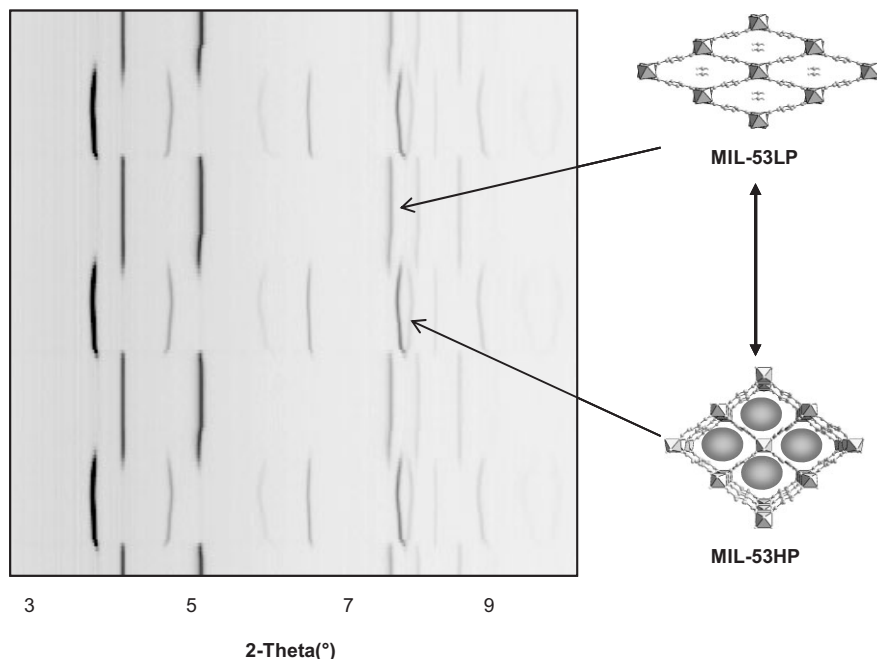


Figure 3. Structural evidences of the cycling ability of the pore opening of MIL-53(Cr) under a CO₂ atmosphere at 293 K.

a monoclinic cell (SG C2/c; $a = 19.713(1) \text{ \AA}$, $b = 8.310(1) \text{ \AA}$, $c = 6.806(1) \text{ \AA}$, $\beta = 105.85(1)^\circ$; $V = 1072.5(1) \text{ \AA}^3$) by using the Dicvol software.^[13] Next, the atomic coordinates of the MIL-53LT phase, without the free water molecules, were used as a starting model and refined by using Fullprof and its graphical interface Winplotr.^[14,15] Fourier difference maps were built using Shextl software^[16] in order to localize the molecules of CO₂ within the pores of MIL-53. Refinement provided good agreement with the experimental data (for crystallographic details see Tables S1 and S2 and Fig. S2 in the Supporting Information). A single CO₂ molecule was localized in the structure with a site occupancy close to 54%. This result was in agreement with other experimental data; specifically, the structure-derived CO₂ content of 2.33 mmol g⁻¹ compared well with the ca. 2–3 mmol g⁻¹ of CO₂ known to be absorbed by MIL-53 during the first step of the adsorption isotherm.

Figure 4a shows the refined structure of MIL-53LP. The topology of the framework remained unchanged compared to MIL-53LT, and the cell parameters are $a = 19.713(1) \text{ \AA}$, $b = 8.310(1) \text{ \AA}$, $c = 6.806(1) \text{ \AA}$, $\beta = 105.85(1)^\circ$; $V = 1072.5(1) \text{ \AA}^3$; SG C2/c. The CO₂ molecules interact with the two opposite chains corresponding to the small diagonal of the rhomblike section of the tunnel (Fig. 4b). The linear CO₂ molecules are lined up along the c -axis (the tunnel direction) with an intermolecular distance $d = 3.4 \text{ \AA}$. This short distance is the same order of magnitude as distances existing in solid CO₂ (3.24–3.57 \AA)^[17] and indicates strong CO₂–CO₂ interactions along the tunnel. Regarding the interactions between CO₂ molecules and the framework, the interatomic distances suggest two scenarios: i) interaction between the carbon atom of

the CO₂ molecule with the oxygen atom of the hydroxyl group of the chain ($d_{\text{C-O}} = 2.80 \text{ \AA}$) and ii) a weak dipolar or quadrupolar interaction between the CO₂ molecule and the hydroxyl group of the framework (the distance between the oxygen atom of the CO₂ molecule and the oxygen atom of the hydroxyl group is close to 3.06 \AA). Interestingly, pore contraction, which occurred in MIL-53 upon adsorption of CO₂ at 1 bar, was slightly lower than in the case of hydration; the unit cell shrunk to 1072 \AA^3 in the case of MIL-53LP compared to ca. 1012 \AA^3 for the water-containing MIL-53LT, which was in agreement with the larger size of CO₂ compared to H₂O.

IR spectroscopic experiments were performed at conditions similar to those used for in situ diffraction studies. CO₂ gas was introduced stepwise from 1 to 10 bar to the activated sample and then progressively removed (Fig. S5, movie). The amount of adsorbed CO₂ could be estimated from the integrated intensity

of the ν_2 CO₂ bands between 645 and 665 cm⁻¹ (Fig. 5b). A profile of the adsorption–desorption curves could be deduced from the evolution of the intensities of these peaks versus pressure (Fig. 5b, top), and it was quite similar to the profile reported from microcalorimetry experiments.^[10] Spectra recorded during an adsorption–desorption cycle provided evidence that the ν_{18a} ring mode^[18] of the terephthalate entities situated at 1022 cm⁻¹ for the dehydrated sample shifted to 1017 cm⁻¹ under 1 bar of CO₂ and progressively returned to its initial position when the pressure increased from 6 to 10 bar (Fig. 5a and Fig. S5). This shift could be directly attributed to the changes in the MIL-53 structure: the bands at 1022 and 1017 cm⁻¹ corresponded to the open and closed forms, respectively. This shift enabled us to evaluate the ratio of the open and closed structures upon CO₂ adsorption (Fig. 5a, top). The resulting diagram was similar to those obtained from the in situ XRD measurements. The adsorption mode of CO₂ could be deduced from the shape of the ν_2 CO₂ band. It is clearly split into two components at 653 and 662 cm⁻¹ under 1 bar CO₂ (Fig. 5b) because of the symmetry lowering of the adsorbed CO₂ molecule. This behavior revealed that the main interaction involves the formation of electron donor–acceptor (EDA) complexes between the C atom of the CO₂ molecule and the electron-donor center of the framework.^[19,20] Moreover, the significant perturbations of both $\nu(\text{OH})$ and $\delta(\text{OH})$ bands of hydroxyl groups upon CO₂ adsorption ($\Delta\nu(\text{OH}) = 22 \text{ cm}^{-1}$ and $\Delta\delta(\text{OH}) = 30 \text{ cm}^{-1}$) were similar to those observed in the case of CO₂–alcohol EDA complexes^[21] and allowed us to identify the electron-donor center as the oxygen atom of the framework hydroxyl groups. For higher

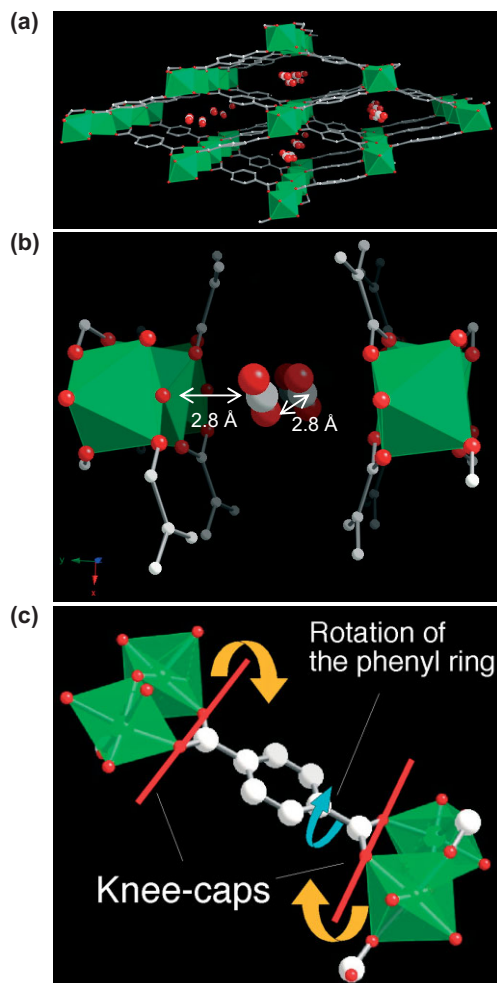


Figure 4. a) View of the refined structure of MIL-53LP along the *c*-axis ($P_{\text{CO}_2}=1$ bar, $T=195$ K); b) closer view of the local interactions between the CO₂ molecules within a channel of MIL-53 ($P_{\text{CO}_2}=1$ bar, $T=195$ K); c) geometrical rearrangement occurring in MIL-53 at the origin of giant breathing. (green: Cr, red: O, light gray: C).

CO₂ pressures (from 5 to 10 bar), a new ν_2 band appeared at 659 cm⁻¹ (Fig. 5b), indicating that the opening of the structure afforded another form of CO₂ adsorption that still perturbed the OH groups ($\Delta\nu(\text{OH})=13$ cm⁻¹ and $\Delta\nu(\text{OH})=15$ cm⁻¹) but to a lesser extent than at low pressure. This second form persisted during the desorption process down to 2–3 bar CO₂, which was the pressure that corresponded to the closing of the structure at the end of the hysteresis loop.

Geometry optimization of the MIL-53LP or “narrow-pore” structure containing 2 CO₂/u.c. (u.c.: unit cell) was performed in parallel by using periodic density functional theory (DFT) calculations with the PW91 functional and the double numerical plus polarization (DNP) basis set, as implemented in the DMol³ code.^[22] The initial atomic coordinates of the framework were taken directly from the refined structure. The resulting arrangement of the CO₂ molecules (Fig. S3) was in good agreement with that obtained experimentally (Fig. 4a), where the CO₂ molecules were situated at the center of the

pore, however with one difference. Whereas simulation suggested an ordered occupation of the tunnels with empty CO₂ sites following the occupied ones along the tunnel, diffraction data suggested disorder or a partial occupation of the CO₂ sites (occupation factor 0.54(1)). The disordered model suggested a random coexistence of the neighboring CO₂ molecules along the channels. Strict order would imply a doubling of the parameters perpendicular to the tunnels, which was not actually observed. Despite this discrepancy, the DFT structure confirmed the presence of the main interaction between the carbon of the CO₂ molecule with the oxygen of the hydroxyl group ($d_{\text{C-O}}=2.9$ Å), which validated the results obtained by using IR spectroscopy. Weak quadrupolar interactions were likely to be present between the CO₂ moieties and the hydroxyl group ($d_{\text{O-H}}=2.3$ Å). In the case of our computational models, these walls were positioned parallel to the *c*-axis of the unit cell. The adsorbate molecules, lying in the same pore, were nearly parallel to each other, and the characteristic distance between two consecutive CO₂ molecules, $d_{\text{C-C}}$, was 3.4 Å. C–O interactions were also present between consecutive CO₂ molecules ($d_{\text{C-O}}=3.15$ Å). In addition, the orientation of the hydroxyl group was slightly modified by interaction with CO₂, as demonstrated by comparing the Cr–O–H angles, which changed by approximately 10% between the optimized CO₂-loaded and unloaded simulated structures. With this adsorption process, there was no significant modification of the remaining framework geometry although small changes by less than 1% were observed for the Cr–O–Cr angles and the Cr–O distances. In order to determine the reason for the structural transition between the HP or “large” and the LP or “narrow” forms of MIL-53, we performed complementary DFT calculations on the HP structure loaded with the same number of CO₂ molecules. The optimized geometry (Fig. S4) favored an arrangement where the adsorbates interacted with the hydroxyl groups on opposite walls of the same pore with nearly parallel CO₂ molecules and characteristic distances $d_{\text{C-C}}=4.4$ Å and $d_{\text{O-H}}=2.2$ Å. Such an interaction would lead to pulling of the pore walls towards each other, thereby moving the CO₂ molecules into the positions observed in our DFT calculations for the LP model.

Therefore, assuming that CO₂ interactions on opposite chains were responsible for shrinking the framework, we ask how the framework could contract so much without falling apart. We recall that shrinking implies atomic movements greater than 5 Å. After reviewing the structure, it became clear that a combination of nondirectional ionic Cr–O bonds with a rigidity of the triangular O–C–O carboxylate group, the O–O axis of each carboxylate acted as a kneecap during the reversible shrinkage (Fig. 4c). Moreover, the free rotation of the C–C bond between the carboxylate groups and the phenyl ring relaxed the tension induced by shrinkage, leading to a stable value of the lattice energy at the end of the process.

Finally, the large breathing effect observed in the MIL-53 structure occurred because the adsorbed species created relatively strong guest–guest bonds along the tunnels, which acted as a backbone for the onset of symmetrical interactions with

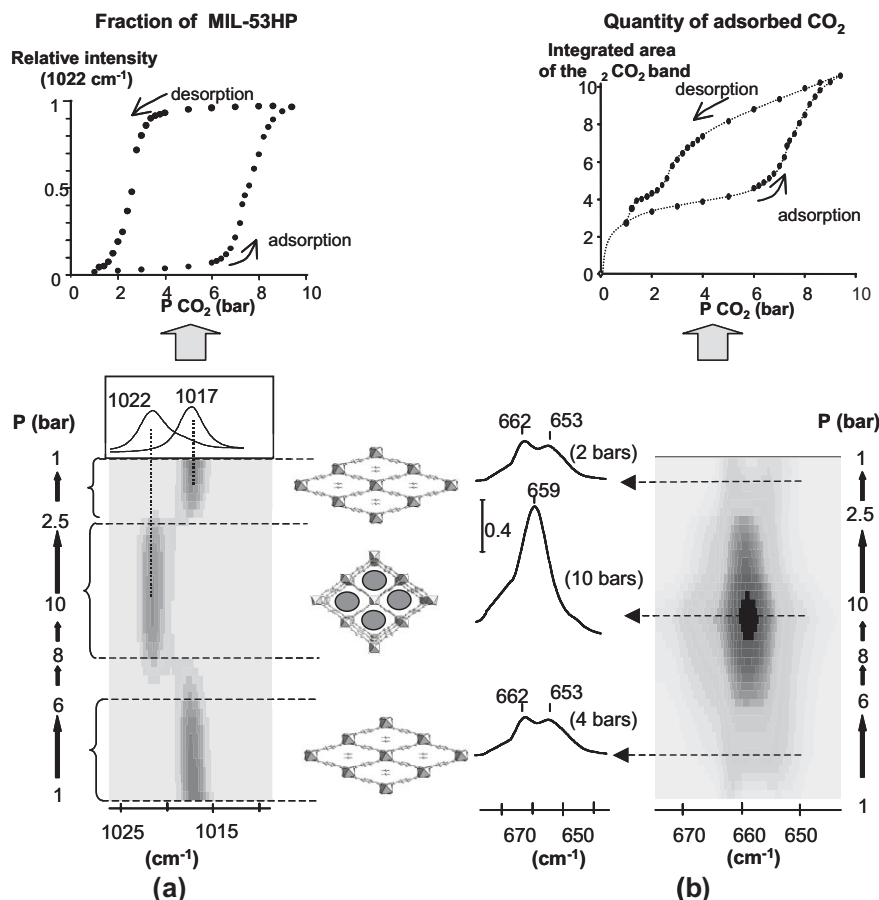


Figure 5. Bottom (2D IR Map): a) Variation in the intensities of MIL-53LP (1017 cm^{-1}) and MIL-53HP (1022 cm^{-1}) bands and b) in the ν_2 CO_2 bands ($653, 662\text{ cm}^{-1}$ MIL-53LP; 659 cm^{-1} MIL-53HP) versus CO_2 pressure. Top: hysteresis phenomenon observed during an adsorption–desorption cycle. Curves were obtained from the quantitative analysis of the corresponding IR spectra.

two opposite chains of the framework (hydrogen bonds when water was involved, dipolar or quadrupolar interactions with CO_2). It is worth noting that whatever the guest (H_2O or CO_2), the existence of OH groups was critical for establishing such interactions. The onset of the interactions forced the evolution of the structure, which was only allowed because the framework possessed some nonrigid sites (weak points) that could accommodate the large variations induced by the strong and diverse host–guest interactions. This also applied to the reopening of the structure under high pressures (>5 bar) up to a maximum filling of the tunnels that was compatible with the elasticity of the framework. At that point, the DFT calculations performed on the loaded HT material indicated that CO_2 molecules interacted directly with the hydroxyl groups. The $\text{O}=\text{C}=\text{O}\cdots\text{H}$ fragment was nearly linear and the characteristic distance $\text{O}(\text{CO}_2)\text{--H}(\text{OH})$ was 2.19 \AA . The predicted structure at higher CO_2 pressures will be the subject of further investigations when a high-pressure cell, such as the one currently under construction at the ESRF, becomes available at the synchrotron facilities.

Experimental

Synthesis: MIL-53 was hydrothermally synthesized by using a modified approach to the previously reported procedure [7]. First, chromium(III) nitrate, terephthalic acid, hydrofluoric acid, and H_2O were mixed in the molar ratio 1:1.5:1:280. Reactants were introduced to a Teflon-lined steel autoclave, and the temperature was set at 493 K for 6 days. A light purple powder was obtained that contained traces of terephthalic acid. The latter was first eliminated by dispersing the powder in an excess of dimethylformamide (DMF) for ca. 10 min with stirring. Next, the free terephthalic acid present in the pores of MIL-53 was evacuated by a solvothermal exchange with DMF (1 g of MIL-53as in 25 mL DMF) by using a Teflon-lined steel autoclave at 423 K overnight. After cooling to room temperature, the solid MIL-53DMF was calcined overnight at 523 K to remove DMF molecules. After cooling in air, the resulting solid adsorbed water at room temperature to give MIL-53LT or $\text{Cr}^{\text{III}}(\text{OH})\cdot(\text{O}_2\text{C-C}_6\text{H}_4\text{-CO}_2)\cdot\text{H}_2\text{O}$.

Adsorption Experiments: CO_2 adsorption analysis was performed at 304 K up to 16 bar. The isotherm was obtained by using an adsorption manometry device with a point-by-point introduction of gas to the sample. Prior to the adsorption experiment, the sample was weighed into the sample cell and placed inside the adsorption manifold without prior outgassing. CO_2 , 99.9999%, was obtained from Air Liquide (Alphagaz, France). Each experiment was repeated several times, and each curve in the figures includes points from at least two experiments.

In Situ Experiments: First, in situ synchrotron powder diffraction experiments were carried out with the RAPID2 [11] powder diffraction detector (material-processing beamline MPW6.2 [12]) at the Synchrotron Radiation Source (Daresbury, UK). A furnace and a capillary gas delivery system, developed at Birkbeck College [23], were used to obtain, in situ, the required starting material—dehydrated MIL-53(Cr)—and to apply smooth gradual changes in CO_2 pressure. Two types of experiments were performed: i) one experiment was conducted with continuous pressure variations (in this case, an approximate rate of 1 bar per 10 s was used from 1 to 10 bar and backwards for several cycles) and ii) the second experiment corresponded to a long experiment in which the CO_2 pressure was increased/decreased from 1 to 10 bar via 1 bar steps of 45 s each. In both cases, diffraction data were collected every 6 s in order to quickly spot structural changes. Experiments were performed at 293 K at $\lambda\sim 1.4\text{ \AA}$. In the second step, another series of in situ synchrotron powder diffraction experiments were performed at the Swiss–Norwegian Beamlines at the ESRF (Grenoble, France). The data were collected on 0.5 mm quartz capillaries filled with sample and attached to a gas manifold by using a MAR345 imaging plate at a sample-to-detector distance of 250 mm, $\lambda=0.71118\text{ \AA}$. Prior to data collection, the MIL-53(Cr) solid was outgassed at 353 K under a primary vacuum until its X-ray powder pattern showed a pure MIL-53HT phase; then, the sample was cooled to 195 K by using a cryostream. Finally, CO_2 was introduced in the capillary, and a high-resolution X-ray powder pattern was collected. The data were integrated by using the Fit2D program (Dr. A. Hammersley, ESRF) and a calibration measurement of a NIST LaB6 standard sample. Uncertainties

in the integrated intensities were calculated at each 2θ point applying Bayesian statistics to the intensity data, considering the geometry of the detector. CO₂ gas (Alphagaz, France, 99.9999% purity) was introduced at each pressure point. The response of the system to the pressure increase was immediate, as seen by in situ powder diffraction. Equilibrium was assumed when two repeatedly measured diffraction patterns became identical.

IR Spectroscopy: Our high pressure cell [24] consisted of a cylinder of stainless steel carrying a toroidal sample holder in its center, where the sample (2 mg), dispersed in deionized water and spread on a silicon wafer, was placed. The heating system guaranteed a maximum temperature of 723 K for the sample, whereas the air-cooling system maintained the two ends of the cell below 573 K in such a way that the tightness (up to 30 bar) could be obtained by using Kalrez O-rings between the external KBr windows and the extremities of the cell. The rest of the space was filled with KBr windows, which limited the dead volume to 0.12 cm³, with the residual space between each sample face and window equal to 0.02 cm. This small dead volume allowed us to limit the contribution of the gas phase to the IR spectra of the adsorbed species. The experiment was carried out at 303 K. Prior to the adsorption experiment, the sample was dehydrated under a primary vacuum at 473 K. The CO₂ pressure was increased from 1 to 10 bar by using stepwise increments of 0.1–1 bar. Equilibrium was assumed when two spectra became identical. IR spectra were recorded with a Nicolet Magna 550 FTIR spectrometer (resolution 2 cm⁻¹).

Computer Simulation: The geometry optimization of the MIL-53(Cr) structure containing 2 CO₂/u.c. and MIL-53LP was performed by using periodic DFT calculations with a PW91 GGA density functional [25] and the double numerical basis set containing polarization functions on hydrogen atoms (DNP) [26] as implemented in the Dmol³ code [22]. The initial atomic coordinates of the hybrid porous framework were taken directly from the refined X-ray structure.

Received: November 20, 2006

Published online: August 2, 2007

- [1] K. Barthelet, J. Marrot, D. Riou, G. Férey, *Angew. Chem. Int. Ed.* **2002**, *41*, 281.
- [2] C. Serre, F. Millange, C. Thouvenot, M. Nogues, G. Marsolier, D. Louër, G. Férey, *J. Am. Chem. Soc.* **2002**, *124*, 13 519.
- [3] S. Kitagawa R. Kitaura, S. Noro, *Angew. Chem. Int. Ed.* **2004**, *43*, 2334.
- [4] K. Uemura, R. Matsuda, S. Kitagawa, *J. Solid State Chem.* **2005**, *178*, 2420.
- [5] S. Kitagawa, K. Uemura, *Chem. Soc. Rev.* **2005**, *34*, 109.
- [6] C. Mellot-Draznieks, C. Serre, S. Surblé, N. Audebrand, G. Férey, *J. Am. Chem. Soc.* **2005**, *127*, 16 273.
- [7] F. Millange, C. Serre, G. Férey, *Chem. Comm.* **2002**, 822.
- [8] T. Loiseau, C. Serre, C. Huguénard, G. Fink, F. Taulelle, M. Henry, T. Bataille, G. Férey, *Chem. Eur. J.* **2004**, *10*, 1366.
- [9] G. Férey, M. Latroche, C. Serre, F. Millange, T. Loiseau, A. Percheron-Guégan, *Chem. Comm.* **2003**, 2976.
- [10] S. Bourrelly, P. L. Llewellyn, C. Serre, F. Millange, T. Loiseau, G. Férey, *J. Am. Chem. Soc.* **2005**, *127*, 13 519.
- [11] A. Berry, W. I. Helsby, B. T. Parker, C. J. Hall, P. A. Buksh, A. Hill, N. Claguea, M. Hillon, G. Corbetta, P. Clifford, A. Tidbury, R. A. Lewis, B. J. Cernik, P. Barnes, G. E. Derbyshire, *Nucl. Inst. Methods in Phys. Res. A* **2003**, *513*, 260.
- [12] R. J. Cernik, P. Barnes, G. Bushnell-Wye, A. J. Dent, G. P. Diakun, J. V. Flaherty, G. N. Greaves, E. L. Heeley, W. Helsby, S. D. M. Jacques, J. Kay, T. Rayment, A. Ryan, C. C. Tang, N. J. Terrill, *J. Synchrotron Radiation* **2004**, *11*, 163.
- [13] A. Boulouf, D. Louër, *J. Appl. Phys.* **1991**, *24*, 987.
- [14] J. Rodriguez-Carvajal, in *Collected Abstracts of Powder Diffraction Meeting*, Toulouse, France **1990**, p. 127.
- [15] T. Roisnel, J. Rodriguez-Carvajal, *Materials Science Forum, Proc. of the European Powder Diffraction Conference (EPDIC 7)* **2001**, *378–381*, 118.
- [16] G. M. Sheldrick, SHELXL97 and SHELXS97, University of Göttingen (Germany) **1997**.
- [17] C. S. Yoo, H. Kohlmann, H. Cynn, M. F. Nicol, V. Iota, T. LeBihan, *Phys. Rev.* **2002**, *B65*, 104 103.
- [18] J. F. Arenas, J. I. Marcos, *Spectrochim. Acta* **1979**, *35A*, 355.
- [19] S. G. Kazarian, M. F. Vincent, F. V. Bright, C. L. Liotta, C. A. Eckert, *J. Am. Chem. Soc.* **1996**, *118*, 1729.
- [20] J. C. Dobrowolski, M. H. Jamroz, *J. Mol. Struct.* **1992**, *275*, 211.
- [21] P. Lalanne, T. Tassaing, Y. Danten, F. Cansell, S. C. Tucker, M. Besnard, *J. Phys. Chem.* **2004**, *A 108*, 2617.
- [22] B. J. Delley, *Chem Phys.* **1990**, *92*, 508. Dmol3, v.4.0, Accelrys, Inc., San Diego **2005**.
- [23] S. D. M. Jacques, O. Leynaud, D. Strusevich, A. M. Beale, G. Sankar, C. M. Martin, P. Barnes, *Angew. Chem. Int. Ed.* **2006**, *45*, 445.
- [24] T. Lesage, C. Verrier, P. Bazin, J. Saussey, M. Daturi, *Phys. Chem. Chem. Phys.* **2003**, *5*, 4435.
- [25] J. P. Perdew, Y. Wang, *Phys. Rev. B* **1986**, *33*, 8822.
- [26] W. J. Hehre, J. H. Ditchfield, J. A. Pople, *J. Chem. Phys.* **1972**, *56*, 2257.